THE DYNAMICAL STRUCTURE OF THE KUIPER BELT AND ITS PRIMORDIAL ORIGIN

Alessandro Morbidelli
Observatoire de la Côte d'Azur

Harold F. Levison
Southwest Research Institute

Rodney Gomes
Observatório Nacional/MCT - Brazil

This chapter discusses the dynamical properties of the Kuiper belt population. Then, it focuses on the characteristics of the Kuiper belt that cannot be explained by its evolution in the framework of the current solar system. We review models of primordial solar system evolution that have been proposed to reproduce the Kuiper belt features, outlining advantages and problems of each of them.

1. Introduction

Since its discovery in 1992, the Kuiper belt has slowly revealed a stunningly complex dynamical structure. This structure has been a gold mine for those of us interested in planet formation because it provides vital clues about this process. This chapter is a review of the current state of knowledge about these issues. It is divided in two parts. The first part (section 2) is devoted to the description of the current dynamics in the Kuiper belt. This will be used in section 3 to highlight the properties of the Kuiper belt population that cannot be explained by the current dynamical processes, but need to be understood in the framework of a scenario of primordial evolution of the outer Solar System. In the second part, we will review the models that have been proposed so far to explain the various puzzling properties of the Kuiper belt. More precisely, section 4 will focus on the origin of the outer edge of the belt; section 5 will describe the effects of the migration of Neptune on the orbital structure of the Kuiper belt objects (KBOs) and section 6 will discuss the origin of the mass deficit of trans-Neptunian population. In section 7 we will present the consequences on the Kuiper belt of a model of the outer Solar System evolution that has been recently proposed to explain the orbital architecture of the planets, the Trojan populations of both Jupiter and Neptune, and the origin of the Late Heavy Bombardment of the terrestrial planets. A general discussion on the current state-of-the-art in Kuiper belt modelling will close the paper in section 8.

2. Current dynamics in the Kuiper belt

Fig. 1 shows a map of the dynamical lifetime of trans-Neptunian bodies as a function of their initial semi-major axis and eccentricity, for an inclination of 1° and with their orbital ellipses oriented randomly (*Duncan et al.*, 1995). Additional maps, referring to different choices of the initial inclination or different projections on orbital element space can be found in *Duncan et al.*, 1995 and *Kuchner et al.*, 2002. These maps have been computed numerically, by simulating the evolution of massless particles from their initial conditions, under the gravitational perturbations of the giant planets. The planets were assumed to be on their current orbits throughout the integrations. Each particle was followed until it suffered a close encounter with Neptune. Objects encountering Neptune would then evolve in the Scattered disk (see *chapter* by *Gomes et al.*).

In fig. 1, the colored strips indicate the timespan required for a particle to encounter Neptune, as a function of its initial semi-major axis and eccentricity. Strips that are colored yellow represent objects that survive for the length of the simulation, 4×10^9 years (the approximate age of the Solar System) without encountering the planet. The figure also reports the orbital elements of the known Kuiper belt objects. Green dots refer to bodies with inclination $i < 4^\circ$, consistent with the low inclination at which the stability map has been computed. Magenta dots refer to objects with larger inclination and are plotted only for completeness.

As the figure shows, the Kuiper belt has a complex dynamical structure, although some general trends can be easily identified. If we denoted the perihelion distance of an orbit by q, and we note that $q = a(1-e)$, where a is the semi-major axis and e is the eccentricity, Fig. 1 shows that most objects with $q \lesssim 35$ AU (in the region $a < 40$ AU) or $q \lesssim$ 37–38 AU (in the region with $42 < a < 50$ AU) are unstable. This is due to the fact that they pass sufficiently close to Neptune to be destabilized. It may be surprising that Neptune can destabilize objects passing at a distance of 5–8 AU, which corresponds to ~ 10 times the radius of Nep-

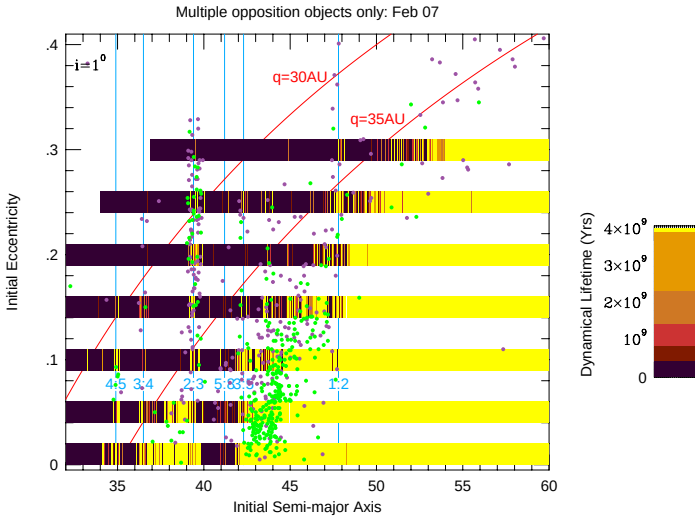

Fig. 1.— The dynamical lifetime for massless particles in the Kuiper belt derived from 4 billion year integrations (*Duncan et al.*, 1995; but extended to $a = 60$ AU for this review). Each particle is represented by a narrow vertical strip of color, the center of which is located at the particle's initial eccentricity and semi-major axis (the initial orbital inclination for all objects was 1 degree). The color of each strip represents the dynamical lifetime of the particle, as reported on the scale on the right hand side. For reference, the locations of the important Neptune mean-motion resonances are shown in blue and two curves of constant perihelion distance, q, are shown in red. The (a, e) elements of the Kuiper belt objects with orbits determined over 3 oppositions are also shown. Green dots are for $i < 4°$, magenta dots otherwise.

tune's gravitational sphere of influence or Hill radius. The instability, in fact, is not due to close encounters with the planet, but to the overlapping of its outer mean motion resonances. It is well known that mean motion resonances become wider at larger eccentricity (see for instance *Dermott and Murray*, 1983 and also *Morbidelli*, 2002) and that resonance overlapping produces large scale chaos (*Chirikov*, 1960). The overlapping of resonances produces a chaotic band whose extent in perihelion distance away from the planet is proportional to the planet mass at the 2/7 power (*Wisdom*, 1980). To date, the most extended analytic calculation of the width of the mean motion resonances with Neptune up to order 50 has been done by D. Nesvorny, and the result -in good agreement with the stability boundary observed in Fig. 1- is published electronically at http://www.boulder.swri.edu/∼davidn/kbmmr/kbmmr.html.

The semi-major axis of the objects that are above the resonance overlapping limit evolves by 'jumps', passing from the vicinity of one resonance to another, mostly during a conjunction with the planet. Given that the eccentricity of Neptune's orbit is small, the *Tisserand parameter*

$$T = \frac{a_N}{a} + 2\sqrt{\frac{a}{a_N}(1-e^2)}\cos i$$

(a_N denoting the semi-major axis of Neptune, a, e, i the semi-major axis, eccentricity and inclination of the object) is approximately conserved. Thus, the eccentricity of the object's orbit has 'jumps' correlated to those of the semi-major axis, and the perihelion distance remains roughly constant. Consequently, the object wanders over the (a, e) plane and is effectively a member of the Scattered disk. In conclusion, the boundary between the black and the colored region in Fig. 1 marks the boundary of the Scattered disk and has a complicated, fractal structure, which justifies the use of numerical simulations in order to classify the objects (see *Chapters* by *Gladman et al.* and *Gomes et al.*).

Not all bodies with $q < 35$ AU are unstable, though. The exception is those objects deep inside low-order mean-motion resonances with Neptune. These objects, despite approaching (or even intersecting) the orbit of Neptune at perihelion, never get close to the planet. The reason for this can be understood with a little algebra. If a body is in a k_N:k resonance with Neptune, the ratio of its orbital period P to Neptune's P_N is, by definition, equal to k/k_N. In this case, and assuming that the planet is on a quasi-circular orbit and the motions of the particle and of the planet are co-planar, the angle

$$\sigma = k_N\lambda_N - k\lambda + (k - k_N)\varpi, \qquad (1)$$

(where λ_N and λ denote the mean longitudes of Neptune and of the object and ϖ is the object's longitude of perihelion) has a time derivative which is zero on average, so that it librates around an equilibrium value, say $\sigma_{\rm stab}$ (see Fig. 2). The radial distance from the planet's orbit is minimized when the object passes close to perihelion. Perihelion passage happens when $\lambda = \varpi$. When this occurs, from (1) we see that the angular separation between the planet and the object, $\lambda_N - \lambda$, is equal to σ/k_N. For small amplitude librations, $\sigma \sim \sigma_{\rm stab}$; because $\sigma_{\rm stab}$ is typically far from 0 see (Fig. 2), we conclude that close encounters cannot occur (*Malhotra*, 1996). Conversely, if the body is not in resonance, σ circulates (Fig. 2). So, eventually it has to pass through 0, which brings the object to be in conjuction with Neptune during its closest approach to the planet's orbit. Thus, close encounters are possible, if the object's perihelion distance is small enough.

For most mean motion resonances, $\sigma_{\rm stab} = 180°$. However, this is not true for the resonances of type 1:k. In these resonances, if the eccentricity of the body is not very small, there are two stable equilibria at $\sigma_{\rm stab} = 180° \pm \delta$, with $\delta \sim 60°$, while $\sigma = 180°$ is an unstable equilibrium (*Message*, 1958; *Beaugé*, 1994; see Fig. 2). Thus, bodies with small amplitudes of libration, necessarily librate asymmetrically in σ relative to the $(0, 2\pi)$ interval. Symmetric librations are possible only for large amplitude librators.

A detailed exploration of the stability region inside the two main mean-motion resonances of the Kuiper belt, the

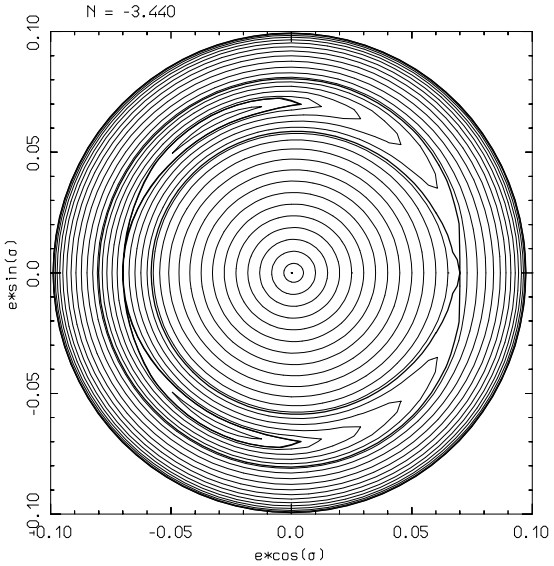

Fig. 2.— The dynamics in the 1:2 resonance with Neptune, in $e\cos\sigma, e\sin\sigma$ coordinates. The motions follow the closed curves plotted in the figure. Librations occur on those curves that do not enclose the origin of the figure. Notice two unstable equilibrium points on the $e\sin\sigma = 0$ line. Each unstable equilibrium is the origin of a critical curve called *separatrix*, plotted in bold in the figure. The one with origin at the unstable point at $\sigma = 0$ separates resonant from not resonant orbits, for which σ respectively librates or circulates. The separatrix with origin at the unstable point in $\sigma = 180^\circ$ delimits two islands of libration around each of the asymmetric stable equilibria.

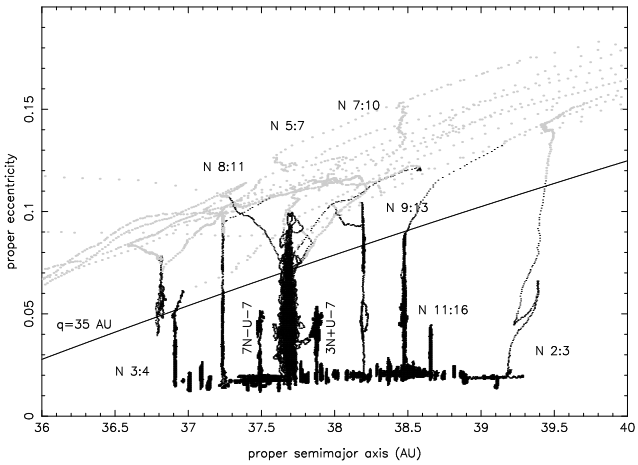

Fig. 3.— The evolution of objects initially at $e = 0.015$ and semi-major axes distributed in the 36.5–39.5 AU range. The dots represent the proper semi-major axis and the eccentricity of the objects –computed by averaging their a and e over 10 My time intervals– over the age of the Solar System. They are plotted in gray after the perihelion has decreased below 32 AU for the first time. Labels Nk_N:k denote the k_N:k two-body resonances with Neptune. Labels k_NN+k_UU+k denote the three-body resonances with Uranus and Neptune, corresponding to the equality $k_N\dot{\lambda}_\mathrm{N}+k_U\dot{\lambda}_\mathrm{U}+k\dot{\lambda} = 0$. Reprinted from *Nesvorný and Roig*, (2001).

2:3 and 1:2 resonances with Neptune, has been done in *Nesvorny and Roig*, 2000, 2001). In general, they found that orbits with large amplitude of libration and moderate to large eccentricities are chaotic, and eventually escape from the resonance, joining the scattered disk population. Conversely, orbits with small eccentricity or small libration amplitude are stable over the age of the Solar System. At large eccentricity, only asymmetric librations are stable in the 1:2 resonance.

Mean motion resonances are not the only important agent structuring the dynamics in the Kuiper belt. In fig. 1, one can see that there is a dark region that extends down to $e = 0$ when $40 < a < 42$ AU. The instability in this case is due to the presence of the secular resonance that occurs when $\dot{\varpi} \sim \dot{\varpi}_N$, where ϖ_N is the perihelion longitude of Neptune. More generally, secular resonances occur when the precession rate of the perihelion or of the longitude of the node of an object is equal to the mean precession rate of the perihelion or the node of one of the planets. The secular resonances involving the perihelion precession rates excite the eccentricities, while those involving the node precession rates excite the inclinations (*Williams and Faulkner*, 1981; *Morbidelli and Henrard*, 1991).

The location of secular resonances in the Kuiper belt has been computed in *Knezevic et al.* (1991). This work showed that both the secular resonance with the perihelion and that with the node of Neptune are present in the $40 < a < 42$ AU region, for $i < 15^\circ$. Consequently, a low-inclination object in this region undergoes large variations in orbital eccentricity so that – even if the initial eccentricity is zero – the perihelion distance eventually decreases below 35 AU, and the object enters the Scattered disk (*Holman and Wisdom*, 1993; *Morbidelli et al.*, 1995). Conversely, a large inclination object in the same semi-major axis region is stable. Indeed, fig. 1 shows that many objects with $i > 4^\circ$ (small dots) are present between 40 and 42 AU. Only large dots, representing low-inclination objects, are absent.

Another important characteristic revealed by Fig. 1 is the presence of narrow regions, represented by brown colored bands, where orbits become Neptune-crossing only after billions of years of evolution. The nature of these weakly unstable orbits remained mysterious for several years. Eventually, it was found (*Nesvorny and Roig*, 2001) that they are, in general, associated either with high order mean-motion resonances with Neptune (i.e. resonances for which the equivalence $k\dot{\lambda} = k_N\dot{\lambda}_N$ holds only for large values of the integer coefficients k, k_N) or three–body resonances with Uranus and Neptune (which occur when $k\dot{\lambda} + k_N\dot{\lambda}_N + k_U\dot{\lambda}_U = 0$ occurs for some integers k, k_N and k_U).

The dynamics of objects in these resonances is chaotic due to the non–zero eccentricity of the planetary orbits. The semi-major axis of the objects remain locked at the corre-

sponding resonant value, while the eccentricity of their orbits slowly evolves. In an (a, e)-diagram like fig. 3, each object's evolution leaves a vertical trace. This phenomenon is called *chaotic diffusion*. Eventually the growth of the eccentricity can bring the diffusing object to decrease the perihelion distance below 35 AU. These resonances are too weak to offer an effective protection against close encounters with Neptune ($\sigma_{\rm stab}/k_N$ is a small quantity because k_N is large), unlike the low order resonances considered above. Thus, once the perihelion distance becomes too low, the encounters with Neptune start to change the semi-major axis of the objects, which leave their original resonance and evolve – from that moment on – in the Scattered disk.

Notice from fig. 3 that some resonances are so weak that, despite forcing the resonant objects to diffuse chaotically, they cannot reach the $q = 35$ AU curve within the age of the Solar System. Therefore, although these objects are not stable from the dynamics point of view, they can be consider that way from the astronomical perspective.

Notice also that chaotic diffusion is effective only for selected resonances. The vast majority of the simulated objects are not affected by any macroscopic diffusion. They preserve their initial small eccentricity for the entire age of the Solar System. Thus, the current moderate/large eccentricities and inclinations of most of the Kuiper belt objects cannot be obtained from primordial circular and coplanar orbits by dynamical evolution in the framework of the current orbital configuration of the planetary system. Likewise, the region beyond the 1:2 mean-motion resonance with Neptune is totally stable up to an eccentricity of ~ 0.3 (Fig. 1). As a result, the absence of bodies beyond 48 AU cannot be explained by current dynamical instabilities. Therefore, these (and other) intriguing properties of the Kuiper belt's structure must, instead, be explained within the framework of the formation and primordial evolution of the Solar System. These topics will be treated in the next sections.

3. Kuiper belt properties acquired during a primordial age

From the current dynamical structure of the Kuiper belt, we conclude that the properties that require an explanation in the framework of the primordial Solar System evolution are:

i) The existence of conspicuous populations of objects in the main mean motion resonances with Neptune (2:3, 3:5, 4:7, 1:2, 2:5, etc.). The dynamical analysis presented above shows that these resonances are stable, but does not explain how and why objects populated these resonances on orbits with eccentricities as large as allowed by stability considerations.

ii) The excitation of the eccentricities in the classical belt, which we define here as the collection of non-resonant objects with $42 < a < 48$ AU and $q > 37$ AU. The median eccentricity of the classical belt is ~ 0.07. It should be noted, however, that the upper eccentricity boundary of this population is set by the long-term orbital stability of the Kuiper belt (see Fig. 1), and thus this semi-major axis region could have contained at some time in the past objects with much larger eccentricities. In any case, even if the current median eccentricity is small, it is nevertheless much larger (an order of magnitude or more) than the one that must have existed when the KBOs formed. The current dynamics are stable, so that, without additional stirring mechanisms, the primordial small eccentricities should have been preserved to modern times.

iii) The peculiar (a, e) distribution of the objects in the classical belt (see Fig. 1). In particular, the population of objects on nearly-circular orbits ($e \lesssim 0.05$) effectively ends at about 44 AU, and beyond this location the eccentricity tends to increase with semi-major axis. If this were simply the consequence of an observational bias that favors the discovery of objects on orbits with smaller perihelion distances, we would expect that the lower bound of the a–e distribution in the 44–48 AU would follow a curve of constant q. This is not the case. Indeed, the eccentricity of this boundary grows more steeply with semi-major axis than this explaination would predict. Thus, the apparent relative under-density of objects at low eccentricity in the region $44 < a < 48$ AU is likely to be a real feature of the Kuiper belt distribution. This under-density cannot be explained by a lack of stability in this region.

iv) The outer edge of the classical belt (Fig. 1). This edge appears to be precisely at the location of the 1:2 mean-motion resonance (MMR) with Neptune. Only large eccentricity objects, typical of the scattered disk or of the detached population (see *Chapter* by *Gladman et al.* for a definition of these populations) seem to exist beyond this boundary (Fig. 1). Again, the under density (or absence) of low eccentricity objects beyond the 1:2 MMR cannot be explained by observational biases (*Trujillo and Brown*, 2001; *Allen et al.*, 2001, 2002; see also *Chapter* by *Kavelaars et al.*). As Fig. 1 shows, the region beyond the 1:2 resonance looks stable, even at moderate eccentricity. So, a primordial distant population should have remained there.

v) The inclination distribution in the classical belt. The observations (see Fig.4) show a clump of objects with $i \lesssim 4^\circ$. However, there are also several objects with much larger inclinations, up to $i \sim 30^\circ$, despite the fact that an object's inclination does not change much in the current Solar System. Observational biases definitely enhance the low inclination clump relative to the large inclination population (the probability of discovery of an object in an ecliptic survey is roughly proportional to $1/\sin(i)$). However, the clump persists even when the biases are taken into account. *Brown* (2001) argued that the debiased inclination distribution is bimodal and can be fitted with two Gaussian functions, one with a standard deviation $\sigma \sim 2^\circ$ for the low-inclination core, and the other with $\sigma \sim 12^\circ$ for the high inclination population (see also *Chapter* by *Kavelaars et al.*). Since the work of Brown, the classical population with $i < 4^\circ$ is

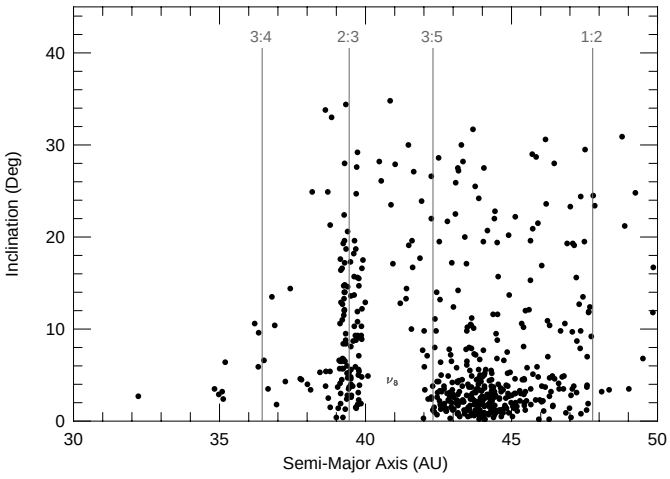

Fig. 4.— The semi-major axis — inclination distribution of all well observed Kuiper belt objects. The important mean motion resonances are also shown.

called the 'cold population', and the remaining one is called the 'hot population' (see *Chapter* by *Gladman et al.* for nomenclature issues).

vi) The correlations between physical properties and orbital distribution. The cluster of low inclination objects visible in the (a, i) distribution disappears if one selects only objects with absolute magnitude $H < 6$ (*Levison and Stern*, 2001)[1]. This implies that intrinsically bright objects are under represented in the cold population. *Grundy et al.* (2005) have shown that the objects of the cold population have a larger albedo, on average, than those of the hot population. Thus, the correlation found by Levison and Stern implies that the hot population contains bigger objects. *Bernstein et al*. (2004) showed that the hot population has a shallower H distribution than the cold population, which is consistent with the absence of the largest objects in the cold belt. In addition, there is a well known correlation between color and inclination (see *Chapter* by *Doressoundiram et al.*). The hot population objects show a wide range of colors, from red to gray. Conversely, the cold population objects are mostly red. In other words, the cold population shows a significant deficit of gray bodies relative to the hot population. The differences in physical properties argue that the cold and the hot populations have different origins.

vii) The mass deficit of the Kuiper belt. The current mass of the Kuiper belt is very small. Estimates range from 0.01 Earth masses ($M_\oplus$) (*Bernstein et al.*, 2004) to 0.1 $M_\oplus$ (*Gladman et al.*, 2001). The uncertainty is due mainly to the conversion from absolute magnitudes to sizes, assumptions about bulk density, and ambiguities in the size distribution (see *Chapter* by *Petit et al.*). Whatever the exact real total mass, there appears to be a significant mass deficit (of 2–3 orders of magnitude) with respect to what models say is needed in order for the KBOs to accrete *in situ*. In particular, in order to grow the objects that we see within a reasonable time (10^7–10^8 My), the Kuiper belt must have consisted of about 10 to 30 $M_\oplus$ of solid material in a dynamically cold disk (*Stern*, 1996; *Stern and Colwell*, 1997a, 1997b; *Kenyon and Luu*, 1998, 1999a, 1999b; *Kenyon and Bromley*, 2004a). If most of the Kuiper belt is currently stable, and therefore objects do not escape, what depleted $\gtrsim 99.9\%$ of the Kuiper belt primordial mass?

All these issues provide us with a large number of clues to understand what happened in the outer Solar System during the primordial era. Potentially, the Kuiper belt might teach us more about the formation of the giant planets than the planets themselves. This is what makes the Kuiper belt so important and fascinating for planetary science.

4. Origin of the outer edge of the Kuiper belt

The existence of an outer edge of the Kuiper belt is very intriguing. Several mechanisms for its origin have been proposed, none of which have resulted yet in a general consensus among the experts in the field. These mechanisms can be grouped in three classes.

Class I: Destroying the distant planetesimal disk It has been argued in *Brunini and Melita* (2002) that a Martian mass body residing for 1 Gy on an orbit with $a \sim 60$ AU and $e \sim 0.15$–0.2 could have scattered most of the Kuiper belt bodies originally in the 50–70 AU range into Neptune-crossing orbits, leaving this region strongly depleted and dynamically excited. It might be possible (see *Chapter* by *Kavelaars et al.*) that the apparent edge at 50 AU is simply the inner edge of such a gap in the distribution of Kuiper belt bodies. A main problem with this scenario is that there are no evident dynamical mechanisms that would ensure the later removal of the massive body from the system. In other words, the massive body should still be present, somewhere in the $\sim 50 - 70$ AU region. A Mars-size body with 4% albedo at 70 AU would have apparent magnitude brighter than 20. In addition, its inclination should be small, both in the scenario where it was originally a Scattered disk object whose eccentricity (and inclination) were damped by dynamical friction (as envisioned by Brunini and Melita), and in the one where the body reached its required heliocentric distance by migrating through the primordially massive Kuiper belt (see *Gomes et al.*, 2004). Thus, in view of its brightness and small inclination, it is unlikely that the putative Mars-size body could have escaped detection in the numerous wide field ecliptic surveys that have been performed up to now, and in particular in that described in *Trujillo and Brown* (2003).

A second possibility for destroying the Kuiper belt beyond the observed edge is that the planetesimal disk was truncated by a close stellar encounter. The eccentricities

[1] The absolute magnitude is the brightness that the object would have if it were viewed at 1 AU, with the observer at the Sun. It relates to size by the formula $LogD^2 = 6.244 - 0.4H - Log(p)$, where D is the diameter in kilometers and p is the albedo.

and inclinations of the planetesimals resulting from a stellar encounter depend critically on a/D, where a is the semi-major axis of the planetesimal and D is the closest heliocentric distance of the stellar encounter (*Ida et al.*, 2000; *Kobayashi and Ida*, 2001). An encounter with a solar-mass star at ~ 200 AU would make most of the bodies beyond 50 AU so eccentric that they intersect the orbit of Neptune, which would eventually produce the observed edge (*Melita et al.*, 2002). An interesting constraint on the time at which such an encounter occurred is set by the existence of the Oort cloud. It was shown in *Levison et al.* (2004) that the encounter had to occur much earlier than ~ 10 My after the formation of Uranus and Neptune, otherwise most of the existing Oort cloud would have been ejected to interstellar space. Moreover, many of the planetesimals in the Scattered disk at that time would have had their perihelion distance lifted beyond Neptune, decoupling them from the planet. As a consequence, the detached population, with $50 \lesssim a \lesssim 100$ AU and $40 < q < 50$ AU, would have had a mass comparable or larger than that of the resulting Oort cloud, hardly compatible with the few detections of detached objects achieved up to now. Finally, this mechanism predicts an correlation between inclination and semi-major axis that is not seen.

A way around the above problems could be achieved if the encounter occurred during the first million years of Solar System history (Levison et al., 2004). At this time, the Sun was still in its birth cluster making such an encounter likely. However, the Kuiper belt objects were presumably not yet fully formed (*Stern*, 1996; *Kenyon and Luu*, 1998), and thus an edge to the belt would form at the location of the disk where eccentricities are ~ 0.05. Interior to this location collisional damping is efficient and accretion can recover from the encounter, beyond this location the objects rapidly grind down to dust (*Kenyon and Broomley*, 2002). If this scenario is true, the stellar passage cannot be responsible exciting the Kuiper belt because the objects that we observe there did not form until much later.

According to the analysis done in *Levison et al.* (2004), an edge-forming stellar encounter should not be the responsible for the origin of the peculiar orbit of Sedna ($a = 484$ AU and $q = 76$ AU), unlike the proposed in *Kenyon and Broomley*, (2004b). In fact, such a close encounter would also produce a relative overabundance of bodies with perihelion distance similar to that of Sedna but with semi-major axes in the 50–200 AU range (*Morbidelli and Levison*, 2004). These bodies have never been discovered, despite the fact that they should be easier to find than Sedna because of their shorter orbital period (see *Chapter* by *Gomes et al.*).

Class II: Forming a bound planetesimal disk from an extended gas-dust disk In *Weidenschilling* (2003), it was shown that the outer edge of the Kuiper belt might be the result of two facts: *i)* accretion takes longer with increasing heliocentric distance and *ii)* small planetesimals drift

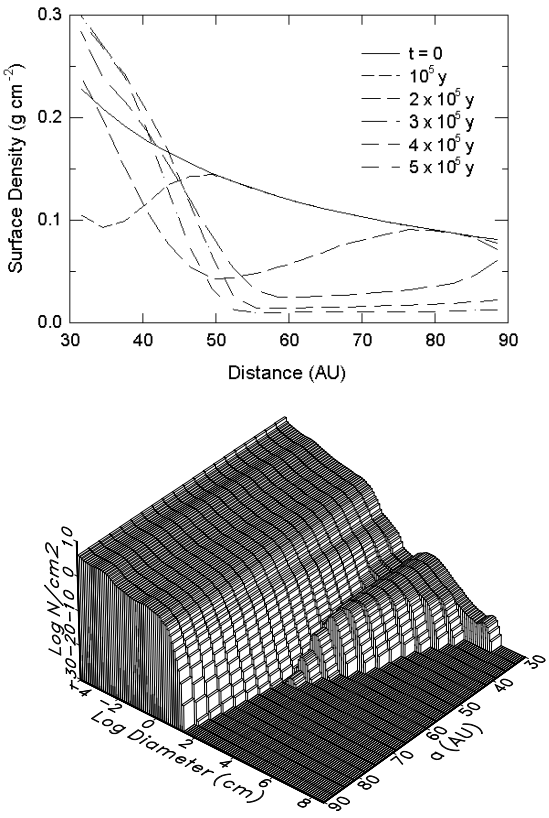

Fig. 5.— Top: the time evolution of the surface density of solids. Bottom: the size distribution as a function of heliocentric distance. From *Weidenschilling* (2003).

inwards due to gas drag. According to Weidenschilling's models, this leads to a steepen of the radial surface density gradient of solids. The edge effect is augmented because, at whatever distance large bodies can form, they capture the ∼meter-sized bodies spiraling inwards from farther out. The net result of the process, as shown by numerical modeling in *Weidenschilling* (2003; see Fig. 5), is the production of an effective edge, where both the surface density of solid matter and the mean size of planetesimals decrease sharply with increasing distance.

A somewhat similar scenario has been proposed in *Youdin and Shu* (2002). In their model, planetesimals formed by gravitational instability, but only in regions of the Solar nebula where the local solid/gas ratio was ~ 3 times that of the Sun (*Sekiya*, 1983). According to the authors, this large ratio occurs because of a radial variation of orbital drift speeds of millimeter-sized particles induced by gas drag. This drift also acts to steeping the surface density distribution of the disk of solids. This means that at some point in the nebula, the solid/gas ratio falls below the critical value to form planetesimals, so that the resulting planetesimal disk would have had a natural outer edge.

A third possibility is that planetesimals formed only within a limited heliocentric distance because of the effect of turbulence. If turbulence in protoplanetary disks

is driven by magneto-rotational instability (MRI), one can expect that it was particularly strong in the vicinity of the Sun and at large distances (where solar and stellar radiation could more easily ionize the gas), while it was weaker in the central, optically thick region of the nebula, known as the 'dead zone' (*Stone et al.*, 1998). The accretion of planetesimals should have been inhibited by strong turbulence, because the latter enhanced the relative velocities of the grains. Consequently, the planetesimals could have formed only in the dead zone, with well defined outer (and inner) edge(s).

Class III: Truncating the original gas disk The detailed observational investigation of star formation regions has revealed the existence of many *proplyds* (anomalously small protoplanetary disks). It is believed that these disks were originally much larger, but in their distant regions the gas was photo-evaporated by highly energetic radiation emitted by the massive stars of the cluster (*Adams et al.*, 2004). Thus, it has been proposed that the outer edge of the Kuiper belt reflects the size of the original Solar System proplyd (*Hollenbach et al.*, 2004).

There is also the theoretical possibility that the disk was born small and did not spread out substantially under its own viscous evolution (*Ruden and Pollack*, 1991). In this case, no truncation mechanism is needed. Observations, however, don't show many small disks, other than in clusters with massive stars.

In all the scenarios discussed above, the location of the edge can be adjusted by tuning the relevant parameters of the corresponding model. In all cases, however, Neptune played no direct role in the edge formation. In this context, it is particularly important to remark (as seen in fig. 1) that the edge of the Kuiper belt appears to coincide precisely with the location of the 1:2 mean-motion resonance with Neptune. This suggests that, whatever mechanism formed the edge, the planet was able to adjust the final location of the outer boundary through gravitational interactions. We will return to this in section 6.2. Notice that a planetesimal disk truncated at ~ 34 AU has been recently postulated in order to explain the dust distribution in the AU Mic system (*Augereau and Beust*, 2006).

5. The role of Neptune's migration

It was shown in *Fernandez and Ip* (1984) that, in the absence of a massive gas disk, while scattering away the primordial planetesimals from their neighboring regions, the giant planets had to migrate in semi-major axis as a consequence of angular momentum conservation. Given the configuration of the giant planets in our Solar System, this migration should have had a general trend (see *Levison et al.*, 2006 for a review). Uranus and Neptune have difficulty ejecting planetesimals onto hyperbolic orbits. Apart from the few percent of planetesimals that can be permanently stored in the Oort cloud or in the Scattered disk, the remaining planetesimals (the large majority) are eventually scattered inwards, towards Saturn and Jupiter. Thus, the ice giants, by reaction, have to move outwards. Jupiter, on the other hand, eventually ejects from the Solar System almost all of the planetesimals that it encounters: thus it has to move inwards. The fate of Saturn is more difficult to predict, *a priori*. However, numerical simulations show that this planet also moves outwards, although only by a few tenths of an AU for reasonable disk's masses (*Hahn and Malhotra*, 1999; *Gomes et al.*, 2004).

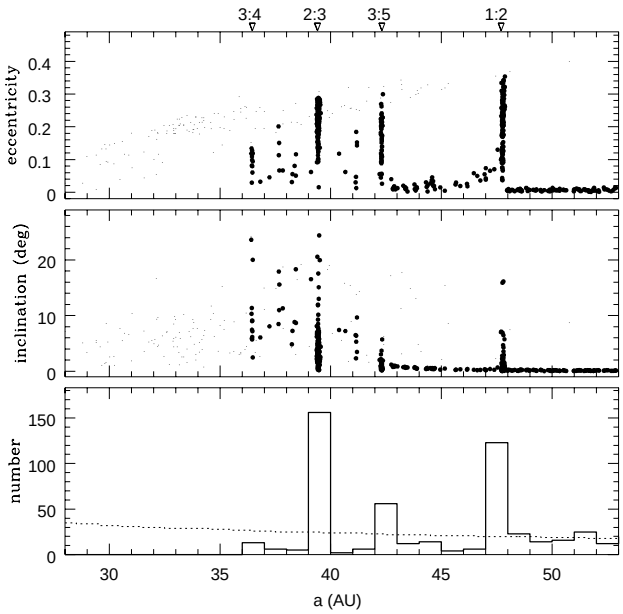

Fig. 6.— The final distribution of Kuiper belt bodies according to the sweeping resonances scenario (courtesy of R. Malhotra). This simulation was done by numerically integrating, over a 200 My time-span, the evolution of 800 test particles on initially quasi-circular and coplanar orbits. The planets are forced to migrate by a quantity Δa (equal to -0.2 AU for Jupiter, 0.8 AU for Saturn, 3 AU for Uranus and 7 AU for Neptune) and approach their current orbits exponentially as $a(t) = a_\infty - \Delta a \exp(-t/4My)$, where a_∞ is the current semi-major axis. Large solid dots represent 'surviving' particles (i.e., those that have not suffered any planetary close encounters during the integration time); small dots represent the 'removed' particles at the time of their close encounter with a planet (e.g. bodies that entered the Scattered disk and whose evolution was not followed further). In the lowest panel, the solid line is the histogram of semi-major axes of the 'surviving' particles; the dotted line is the initial distribution. The locations of the main mean-motion resonances are indicated above the top panel.

5.1. The resonance sweeping scenario

In *Malhotra* (1993, 1995) it was realized that, following Neptune's migration, the mean-motion resonances with Neptune also migrated outwards, sweeping through the primordial Kuiper belt until they reached their present posi-

tions. From adiabatic theory (see for instance *Henrard*, 1982), some of the Kuiper belt objects over which a mean-motion resonance swept, were captured into resonance; they subsequently followed the resonance through its migration, with ever increasing eccentricities. In fact, it can be shown (*Malhotra*, 1995) that, for a $k_N : k$ resonance, the eccentricity of an object grows as

$$\Delta e^2 = \frac{(k - k_N)}{k} \log \frac{a}{a_i} ,$$

where a_i is the semi-major axis that the object had when it was captured in resonance and a is its current semi-major axis. This relationship neglects secular effects inside the mean motion resonance, that can be important if Neptune's eccentricity is not zero and its precession frequencies are comparable to those of the resonant particles (*Levison and Morbidelli*, 2003). This model can account for the existence of the large number of Kuiper belt objects in the 2:3 mean-motion resonance with Neptune (and also in other resonances), and can explain their large eccentricities (see fig. 6). Assuming that all objects were captured when their eccentricities were close to zero the above formula indicates that, Neptune had to have migrated ~ 7 AU in order to reproduce quantitatively the observed range of eccentricities (up to ~ 0.3) of the resonant bodies.

In *Malhotra* (1995), it was also shown that the bodies captured in the 2:3 resonance can acquire large inclinations, comparable to those of Pluto and other objects. The mechanisms that excite the inclination during the capture process have been investigated in detail in *Gomes* (2000), who concluded that, although large inclinations can be achieved, the resulting proportion of high inclination versus low inclination bodies, as well as their distribution in the e–i plane, does not reproduce the observations well. We will return to this issue in section 5.2.

The mechanism of adiabatic capture into resonance requires that Neptune's migration happened very smoothly. If Neptune had encountered a significant number of large bodies, its jerky migration would have jeopardized the capture into resonances. For instance, direct simulations of Neptune's migration in *Hahn and Malhotra* (1999) – which modeled the disk with Lunar to Martian-mass planetesimals – did not result in any permanent captures. Adiabatic captures into resonance can be seen in numerical simulations only if the disk is modeled using many more planetesimals with smaller masses (*Gomes*, 2003; *Gomes et al.*, 2004). The constraint set by the capture process on the maximum size of the planetesimals that made up the bulk of the mass in the disk has been recently estimated in *Murray-Clay and Chiang* (2006). They found that resonance capture due to Neptune's migration is efficient if the bulk of the disk particles was smaller than ~ 100 km and the fraction of disk mass in objects with sizes $\gtrsim 1000$ km was less than a few percent. This result appears too severe, because the results in *Gomes*, (2003) and *Gomes et al.*, (2004) show that resonant captures occur in disks entirely constructed of Pluto-mass objects, although probably with a smaller efficiency than required in Murray-Clay and Chiang's work.

If migration really happened smoothly, *Murray-Clay and Chiang* (2006) worked out a constraint on the migration rate. Remember that there are two islands of libration in the 1:2 resonance with Neptune (see Fig. 2). If Neptune's migration occurs in less than 10 My, they showed that objects captured in the 1:2 resonance should preferentially be in the trailing island (that wehre σ librates around a value $\sigma_{\rm stab} > \pi$). Converesely, most of the observed objects are in the leading island. This, at first sight, points to a slow Neptune's migration. As we will see below, however, resonant objects can be captured also from the scattered disk, and Neptune's migration might have been very different from what was originally envisioned. Thus, it is unclear which kind of constraint is provided by the internal distribution of the 1:2 resonant objects.

As shown in Fig. 6, if the resonance sweeping scenario can explain the existence of the resonant populations, it cannot explain the orbital distribution in the classical belt, between 40 and 48 AU, nor the mass depletion of the Kuiper belt. The eccentricity excitation and, in particular, the inclination excitation obtained in the simulation in that region are far too small compared to those inferred from the observations. Thus, *Hahn and Malhotra* (2005) suggested that resonance sweeping occurred after that some perturbation excited, and perhaps depleted, the planetesimal disk. Thus, the eccentricity and inclination distribution in the classical belt would not have been sculpted by the sweeping process, but would be the relic of such previous excitation mechanism(s). A similar conclusion was reached recently by *Lykawka and Mukai* (2007a), who found that the populations of objects in distant mean motion resonances with Neptune (i.e. with $a > 50$ AU) and their eccentricity-inclination-libration amplitude distributions can be explained by resonance sweeping only if the disk in the 40-48 AU region was already pre-excited in both e and i. Possible mechanisms of excitation and their problems will be briefly discussed in sect. 6.

5.2. The origin of the hot population

The observation that the largest objects in the hot population are bigger than those in the cold population lead *Levison and Stern*, (2001) to suggest that the hot population formed closer to the Sun and was transported outward during the final stages of planet formation. *Gomes* (2003) showed that the simple migration of Neptune described in the previous section could accomplish this feat.

In particular, *Gomes* (2003) studied the migration of the giant planets through a disk represented by $10,000$ particles, a much larger number than had previously been attempted. In Gomes' simulations, during its migration Neptune scattered the planetesimals and formed a massive Scattered disk. Some of the scattered bodies decoupled from the planet, decreasing their eccentricities through interactions with some secular or mean-motion resonance (see *Chapter* by *Gomes et al.* for a detailed discussion of how resonances

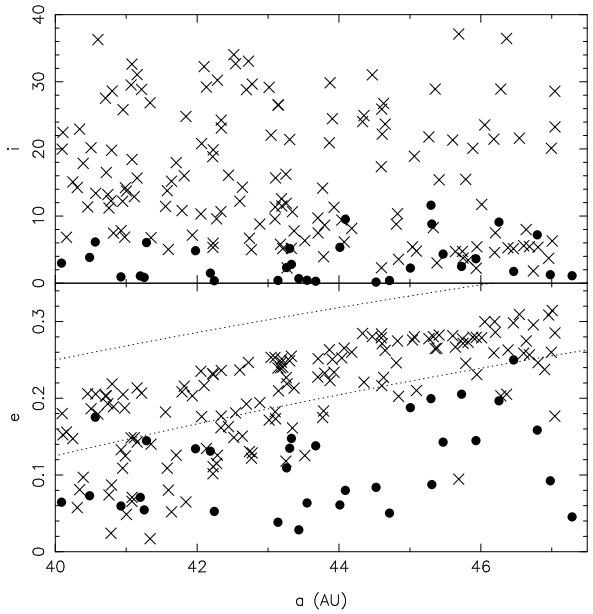

Fig. 7.— The orbital distribution in the classical belt according to the simulations in *Gomes* (2003). The dots denote the population that formed locally, which is only moderately dynamically excited. The crosses denote the bodies that were originally inside 30 AU. Therefore, the resulting Kuiper belt population is the superposition of a dynamically cold population and a dynamically hot population, which gives a bimodal inclination distribution. The dotted curves in the eccentricity vs. semi-major axis plot correspond to $q = 30$ AU and $q = 35$ AU.

can decrease the eccentricities). If Neptune were not migrating, the decoupled phases would have been transient. In fact, the dynamics are reversible, so that the eccentricity would have eventually increased back to Neptune-crossing values. However, Neptune's migration broke the reversibility, and some of the decoupled bodies managed to escape from the resonances and remained permanently trapped in the Kuiper belt. As shown in fig. 7, the current Kuiper belt would therefore be the result of the superposition in (a, e)-space of these bodies with the local population, originally formed beyond 30 AU.

The local population stayed dynamically cold, in particular in inclination, because its objects were only moderately excited by the resonance sweeping mechanism, as in fig. 6. Conversely, the population captured from the scattered disk had a much more extended inclination distribution, for two reasons:*(i)* the inclinations got excited during the scattered disk phase before capture and *(ii)* there was a dynamical bias in favor of the capture of high-inclination bodies, because at large-i the ability of mean motion resonances to decrease the eccentricity is enhanced (see *Chapter* by *Gomes et al.*). Thus, in Gomes model the current cold and hot populations should be identified respectively with the local population and with the population trapped from the scattered disk.

This scenario is appealing because, assuming that the bodies' color varied in the primordial disk with heliocentric distance, it qualitatively explains why the scattered objects and hot classical belt objects – which mostly come from regions inside $\sim$30 AU – appear to have similar color distributions, while the cold classical objects – the only ones that actually formed in the trans-Neptunian region – have a different distribution. Similarly, assuming that at the time of Neptune's migration the maximum size of the objects was a decreasing function of their initial heliocentric distance, the scenario also explains why the biggest Kuiper belt objects are all in the hot population.

As Fig. 7 shows, there may be some quantitative problems in the reproduction of the orbital distribution of the hot Kuiper belt in Gomes scenario (for instance the perihelion distances appear to be somewhat too low). However, an issue of principle concerns the relative weight between the hot and cold populations. In Gomes's simulations, only a fraction of a percent of the original scattered disk remained trapped in the hot population. On the other hand, the cold population was not depleted by the resonance sweeping, so that it retained most of the original objects. Thus, if the local population was similar in size distribution and number density to the planetesimal disk from which the scattered disk was extracted, it should outnumber the hot population by a huge factor (of ~ 1000). So, in order to obtain a final inclination distribution that quantitatively reproduces the debiased inclination distribution of *Brown* (2001), Gomes had to scale down the number of objects in the cold population by an appropriate factor, assuming that some mechanism, not included in the simulation, caused a decimation, and hence a mass depletion, of the local population. These mechanisms are reviewed in the next section.

Before concluding this section, we note that the work by *Gomes* (2003) also have important implications for the origin of the detached population. This issue is addressed in detail in the *Chapter* by *Gomes et al.* and therefore we do not discuss it here.

6. The mass deficit problem

As we described in section 3, the Kuiper belt only contains roughly 0.1% of the mass that is required to grow the objects that we see. So, the natural question is what happened to all that mass. We refer to this issue as the 'mass deficit problem.' We now review ideas that are currently in the literature.

6.1. Mass removal

Two general scenarios have been proposed for the mass depletion: *(i)* a strong dynamical excitation of the Kuiper belt, which caused the ejection of most of the bodies from the Kuiper belt to the Neptune-crossing region, and *(ii)* the collisional comminution of most of the mass of the Kuiper belt into dust. We start our discussion with (i).

Because dynamics are size-independent, a dynamical depletion scenario requires that the primordial population in

the Kuiper belt had a size distribution similar to the one that (currently) exists, but with a number of objects at each size multiplied by the ratio between the primordial mass and the current mass. Remember that, in the current Solar System configuration, most of the Kuiper belt is stable, so that dynamical erosion cannot signficantly reduce the total number of objects. The idea is, therefore, that some perturbation, that acted in the past and is no-longer at work, strongly excited the orbital distribution of the Kuiper belt population. Most of the original objects acquired Neptune-crossing eccentricities, so that they were subsequently eliminated by the scattering action of the planets. Only a small fraction of the original population, corresponding to the surviving mass fraction, remained in the Kuiper belt on excited orbits like those of the observed objects. Thus, this scenario aims at explaining at the same time the mass depletion of the Kuiper belt and its orbital excitation.

A first dynamical depletion mechanism was proposed in *Morbidelli and Valsecchi* (1997) and later revisited in *Petit et al.* (2001). This mechanisms invokes the existence of a planetary embryo, with mass comparable to that of Mars or the Earth, in the scattered disk for $\sim 10^8$ y. Another mechanism was proposed by *Nagasawa et al.* (2000) and invokes the sweeping of secular resonances through the Kuiper belt during the dispersion of the primordial gas disk.

The problem with the dynamical depletion scenario, which was not immediately recognized, is that the ejection of a massive population of objects from the Kuiper belt to the Neptune-crossing region would cause Neptune to migrate into the Kuiper belt. After all, this scenario invokes a $\sim 15\,M_\oplus$ object to remove $\gg 15\,M_\oplus$ of disk material and angular momentum must be conserved. For instance, revisiting the *Petit et al*. (2001) work with simulations that account for the effect of the planetesimals on the dynamics of the massive bodies, *Gomes et al*. (2004) showed that even a disk containing $\sim 4\,M_\oplus$ of material between 40 and 50 AU drives Neptune beyond 30 AU. This is much less than the mass required (10–30 $M_\oplus$) by models of the accretion of Kuiper belt bodies (*Stern and Colwell*, 1997a; *Kenyon and Luu*, 1999b).

The sole possibility for a viable dynamical model of Kuiper belt depletion is if the objects were kicked directly to hyperbolic or Jupiter-crossing orbits and were eliminated without interacting with Neptune. Only the passage of a star through the Kuiper belt seems to be capable of such an extreme excitation (*Kobayashi et al.*, 2005). However, the cold Kuiper belt would not survive in this case.

We note in passing that, even if we ignore the problem of Neptune's migration, massive embryos or secular resonance sweeping are probably not able to reproduce the inclination distribution observed in the Kuiper belt. Thus, these mechanisms are unlikely to be an alternative to the scenario proposed in *Gomes* (2003) for producing the hot classical belt. Consequently, the idea of *Hahn and Malhotra* (2005) and *Lykawka and Mukai* (2007a) that the classical belt acquired its current excitation before Neptune's migration is not supported, so far, by an appropriate excitation mechanism.

The collisional grinding scenario was proposed in *Stern and Colwell* (1997b) and *Davis and Farinella* (1997, 1998), and then pursued in *Kenyon and Luu* (1999a) and *Kenyon and Bromley* (2002, 2004a). It is reviewed in detail in the *Chapter* by *Kenyon et al.*. In essence, a massive Kuiper belt with large eccentricities and inclinations would experience very intense collisional grinding. Consequently, most of the mass originally in bodies smaller than several tens of kilometers could be comminuted into dust, and then evacuated by radiation pressure and Poynting-Robertson drag. This would lead to a substantial depletion in mass.

To work, the collisional erosion scenario requires that two essential conditions be fulfilled. First, it requires a peculiar primordial size distribution, such that all of the missing mass was contained in small, easy-to-break objects, while the number of large objects was essentially identical to that in the current population. Some models support the existence of such a size distribution at the end of the accretion phase (*Kenyon and Luu*, 1998, 1999b). However, there are several arguments in favor of a completely different size distribution in the planetesimal disk. The collisional formation of the Pluto–Charon binary (*Canup*, 2005) and of the 2003 EL_{61} family (*Barkume et al.*, 2006), the capture of Triton onto a satellite orbit around Neptune (*Agnor and Hamilton*, 2006), and the fact that the Eris, the largest known Kuiper belt object, is in the detached population (*Brown et al.*, 2005), suggest that the number of big bodies was much larger in the past, with as many as 1,000 Pluto-sized objects (*Stern*, 1991). Moreover, we have seen above that the mechanism of *Gomes* (2003) for the origin of the hot population also requires a disk's size distribution with $\sim 1,000$ times more large objects than currently present in the Kuiper belt. Finally, *Charnoz and Morbidelli* (2007) showed that, if the size distribution required for collisional grinding in the Kuiper belt is assumed for the entire planetesimal disk (5-50 AU), the Oort cloud and the scattered disk would not contain enough comet-size objects to supply the observed fluxes of long-period and Jupiter-family comets: the cometesimals would have been destroyed before being stored in the comet reservoirs (also see *Stern and Weissman* 2001). So, to fulfill all these constraints and still have an effective collisional grinding in the Kuiper belt, one has to assume that the size distribution were totally different in the region of the proto-planet disk swept by Neptune and in the region of the disk that became the Kuiper belt. This, *a priori*, seems unlikely, given the proximity between the two regions; however, we will come back to this in sect. 8.

The second essential condition for substantial collisional grinding is that the energy of collisions is larger than the energy required for disruption of the targets. Thus, either the KBOs are extremely weak (the successful simulations in *Kenyon and Bromley* (2004) had to assume a specific energy for disruption that is at least an order of magnitude lower than predicted by the hydrodynamical, in particular smooth-particle hydrodynamical (SPH), simulations of fragmentation by *Benz and Asphaug*, 1999), or the massive primordial Kuiper belt had a large dynamical excitation, with $e \sim 0.25$

and/or $i \sim 7^\circ$ (as assumed in *Stern and Colwell*, 1997b). However, if, as we argued above, the hot population was implanted in the Kuiper belt via the low efficiency process of *Gomes*, (2003), then it was never very massive and would not have had much effect on the collisional evolution of the cold population. Thus, the cold population must have ground itself down. This is unlikely because the excitation of the cold-population is significantly smaller than the required values reported above. There is the possibility that the collisional erosion of the cold belt was due to the high-velocity bombardment by projectiles in the scattered disk. The scattered disk was initially massive, but its dynamical decay was probably too fast (~ 100 My, see *Duncan and Levison*, 1997). The collisional action of the scattered disk onto the cold belt was included in *Charnoz and Morbidelli* (2007) but turned out to be a minor contribution.

6.2. Pushing out the Kuiper belt

Given the problems explained just above, an alternative way of solve the mass deficit problem was proposed in *Levison and Morbidelli* (2003). In this scenario, the primordial edge of the massive protoplanetary disk was somewhere around 30–35 AU and the *entire* Kuiper belt population – not only the hot component as in *Gomes* (2003) – formed within this limit and was transported to its current location during Neptune's migration. The transport process for the cold population had to be different from the one found in *Gomes* (2003) for the hot population (but still work in parallel with it), because the inclinations of the hot population were excited, while those of the cold population were not.

In the framework of the classical migration scenario (*Malhotra*, 1995; *Gomes et al.*, 2004), the mechanism proposed in *Levison and Morbidelli* (2003) was the following: the cold population bodies were initially trapped in the 1:2 resonance with Neptune; then, as they were transported outwards by the resonance, they were progressively released due to the non-smoothness of the planetary migration. In the standard adiabatic migration scenario (*Malhotra*, 1995), there would be a resulting correlation between the eccentricity and the semi-major axis of the released bodies. However, this correlation was broken by a secular resonance embedded in the 1:2 mean-motion resonance. This secular resonance was generated by the objects in the resonance, themselves. In particular, unlike previous studies of migration, Levison and Morbidelli included the mass of the objects in the resonance, which modified the precession rate of Neptune's orbit.

Simulations of this process matched the observed (a, e) distribution of the cold population fairly well, while the initially small inclinations were only very moderately perturbed. In this scenario, the small mass of the current cold population is simply due to the fact that only a small fraction of the massive disk population was initially trapped in the 1:2 resonance and then released on stable non-resonant orbits. The final position of Neptune would simply reflect the primitive truncation of the protoplanetary disk (see *Gomes et al.*, 2004 for a more detailed discussion). Most importantly, this model explains why the current edge of the Kuiper belt is at the 1:2 mean-motion resonance with Neptune, despite the fact that none of the mechanisms proposed for the truncation of the planetesimal disk involves Neptune in a direct way (see section 4). The location of the edge was modified by the migration of Neptune, via the migration of the 1:2 resonance.

On the flip side, the model in *Levison and Morbidelli* 2003) re-opened the problem of the origin of the different physical properties of the cold and hot populations, because both would have originated within 35 AU, although in somewhat different parts of the disk. Moreover, *Lykawka and Mukai* (2007a) showed that this model cannot reproduce the low-to-moderate inclination objects in the distant (i.e. beyond 50 AU) high-order mean motion resonances with Neptune.

7. Effects of a Dynamical Instability in the Orbits of Uranus and Neptune

The models reviewed in the previous sections assume that Neptune migrated outward on a nearly-circular orbit. However, a substantially different model of the evolution of the giant planets has been recently proposed. This model –often called the 'Nice model'– reproduces, for the first time, the orbital architecture of the giant planet system (orbital separations, eccentricities, inclinations; *Tsiganis et al.*, 2005) and the capture of the Trojan populations of Jupiter (*Morbidelli et al.*, 2005) and Neptune (*Tsiganis et al.*, 2005; *Sheppard and Trujillo*, 2006). It also naturally supplies a trigger for the Late Heavy Bombardment (LHB) of the terrestrial planets (*Gomes et al.*, 2005), and quantitatively reproduces most of the LHB's characteristics.

In the Nice model, the giant planets are assumed to be initially on nearly-circular and coplanar orbits, with orbital separations significantly smaller than the ones currently observed. More precisely, the giant planet system is assumed to lie in the region from ~ 5.5 AU to ~ 14 AU, and Saturn is assumed to be closer to Jupiter than their mutual 1:2 MMR. A planetesimal disk is assumed to exist beyond the orbits of the giant planets, on orbits whose dynamical lifetime is at least 3 My (the supposed lifetime of the gas-disk). The outer edge of the planetesimal disk is assumed to lie at ~ 34 AU and the total mass is $\sim 35 M_\oplus$ (see Fig. 8a).

With the above configuration, the planetesimals at the inner edge of the disk evolve onto Neptune-scattering orbits on a timescale of a few million years. Consequently, the migration of the giant planets proceeds at very slow rate, governed by the slow planetesimal escape rate from the disk. Because the planetary system would be stable in absence of interactions with the planetesimals, this slow migration continues for a long time, slightly damping out as the unstable disk particles are removed from the system (Fig. 8). After a long time, ranging from 350 My to 1.1 Gy in the simulations of *Gomes et al.* (2005) — which is consistent with the timing of the LHB, approximately 650 My after planet

formation — Jupiter and Saturn eventually cross their mutual 1:2 mean-motion resonance (Fig. 8b). This resonance crossing excites their eccentricities to values slightly larger than those currently observed. The small jump in Jupiter's and Saturn's eccentricities drives up the eccentricities of Uranus and Neptune, however. The ice giant's orbits become chaotic and start to approach each other. Thus, a short phase of encounters follows the resonance-crossing event. Consequently, both ice giants are scattered outward, onto large eccentricity orbits ($e \sim$ 0.3–0.4) that penetrate deeply into the disk (Fig. 8c). This destabilizes the full planetesimal disk and disk particles are scattered all over the Solar System. The eccentricities of Uranus and Neptune and –to a lesser extent– of Jupiter and Saturn, are damped on a timescale of a few My due to the dynamical friction exerted by the planetesimals. Thus, the planets decouple from each other, and the phase of mutual encounters rapidly ends. During and after the eccentricity damping phase, the giant planets continue their radial migration, and eventually reach final orbits when most of the disk has been eliminated (Fig. 8d).

The temporary large eccentricity phase of Neptune opens a new degree of freedom for explaining the orbital structure of the Kuiper belt. The new key feature to the dynamics is that, when Neptune's orbit is eccentric, the full (a, e) region up to the location of the 1:2 resonance with the planet is chaotic, even for small eccentricities. This allows us to envision the following scenario. We assume, in agreement with several of the simulations of the Nice model, that the large eccentricity phase of Neptune is achieved when the planet has a semi-major axis of ~ 28 AU, after its last encounter with Uranus. In this case, a large portion of the current Kuiper belt is already interior to the location of the 1:2 resonance with Neptune. Thus, it is unstable, and can be invaded by objects coming from within the outer boundary of the disk (i.e. $\lesssim$34 AU). When the eccentricity of Neptune damps out, the mechanism for the onset of chaos disappears. The Kuiper belt becomes stable, and the objects that happen to be there at that time remain trapped for the eternity. Given that the invasion of the particles is fast and the damping of Neptune's eccentricity is also rapid, there is probably not enough time to excite significantly the particles' orbital inclinations if Neptune's inclination is also small. Therefore, we expect that this mechanism may be able to explain the observed cold population. The hot population is then captured later, when Neptune is migrating up to its final orbit on a low-eccentricity orbit, as in *Gomes* (2003).

The numerical simulations of this process have been presented in *Levison et al*. (2007). Fig. 9 compares with the observations the semi-major axis vs. eccentricity distribution resulting from one of the simulations, 1 Gy after the giant planet instability. The population of quasi-circular objects at low inclination extends to ~ 45 AU, in nice agreement with the observations. The deficit of low eccentricity objects between 45 and 48 AU is reproduced, and the outer edge of the classical belt is at the final location of the 1:2

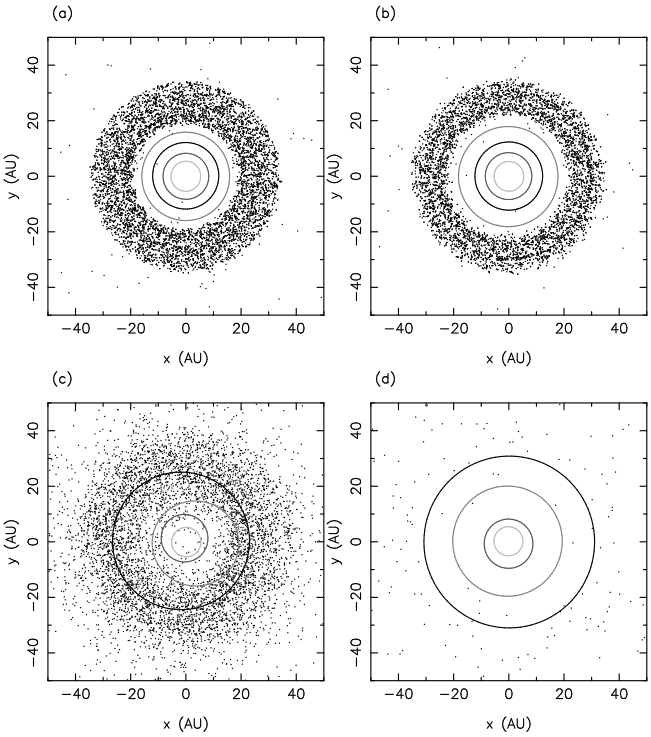

Fig. 8.— Solar System evolution in the Nice model. (a): at a time close to the beginning of the evolution. The orbits of the giant planets (concentric circles) are very close to each other and are quasi-circular. They are surrounded by a disk of planetesimals, whose inner edge is due to the perturbations from the planets and the outer edge is assumed to be at 34 AU. (b): immediately before the great instability. Saturn is about crossing the 1:2 resonance with Jupiter. (c): at the time of the instability. Notice that the orbits of the planets have become eccentric and now penetrate the planetesimal disk. (d): after the LHB. The planets are parked on orbits very similar (in terms of separation, eccentricity, and inclination) to their current ones. The massive planetesimal disk has been destroyed. Only a small fraction of the planetesimals remain in the system on orbits typical of the scattered disk, Kuiper belt, and other small body reservoirs. From *Gomes et al.* (2005).

MMR with Neptune as observed. Moreover, the real Kuiper belt shows a population of objects with $q \sim 40$ AU beyond the 1:2 resonance with Neptune, which are known to be stable (*Emelýanenko et al*. 2003). This population has been known by several names in the literature, which include the fossilized scattered disk, the extended scattered disk, and the detached population (see *Chapter* by *Gladman et al.*). This model reproduces this population quite well.

Three main differences are also noticeable, though. *(i)* All the mean motion resonances are overpopulated relative to the classical belt. This is probably the consequence of the fact that in the simulations the migration of Neptune's orbit and its eccentricity damping were forced smoothly, through fake analytic terms of the equations of motion. As we said

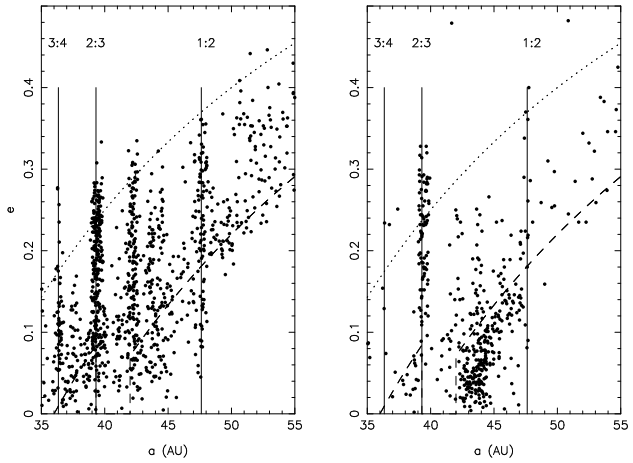

Fig. 9.— The distribution of semi major axes and eccentricities in the Kuiper belt. Left panel: result of a simulation based on the Nice model. Right panel: the observed distribution (3 oppositions objects only). The vertical solid lines mark the main resonance with Neptune. The dotted curve denotes perihelion distance equal to 30 AU and the dashed curve delimits the region above which only high inclination objects or resonant objects can be stable over the age of the Solar System.

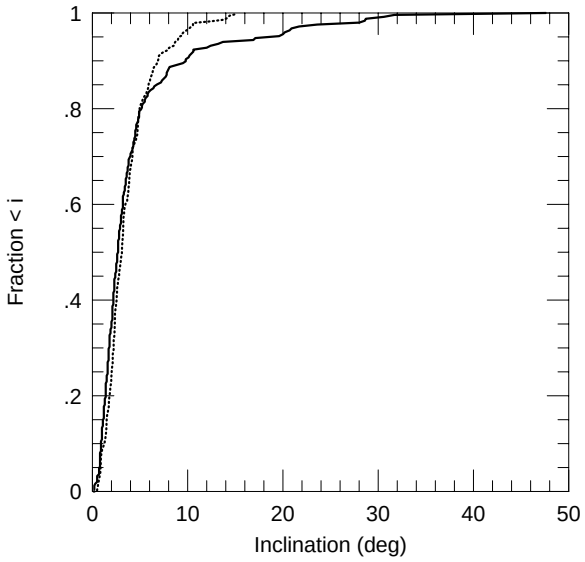

Fig. 10.— The cumulative inclination distribution of the observed classical belt objects (solid curve) and that expected from the result of our simulation, once the observational biases are taken into account (dotted curve).

above, a migration with some stochastic component (due to the encounters with massive objects in the disk) would have produced fewer surviving bodies in the resonances. *(ii)* The region above the long-dashed curve is overpopulated in the simulation. The curve represents approximately the boundary between the stable (yellow) and the unstable (black) regions in Fig. 1. Thus, if the final orbits of the giant planets were exactly the same as the real ones and the simulations were extended for the age of the Solar System, most of the population above the curve would be depleted as a consequence of chaotic dynamics. *(iii)* The cold Kuiper belt has eccentricities that are slightly too large. The median eccentricity of the real objects with $42 < a < 48$ AU and $q > 37$ AU is 0.07, while the model produces a value of 0.10.

Figure 10 shows the cumulative inclination distribution of objects trapped in the classical belt at the end of a simulation and compares it with the observed distribution. For the comparison to be meaningful, the simulated distribution was run through a survey bias-calculator, following the approach of *Brown* (2001). The two curves are very similar. Indeed, they are almost indistinguishable for inclinations less then 6 degrees. This means that the cold population, and the inclination distribution within it, has been correctly reproduced, as well as the distribution in the lower part of the hot population (i.e. that with $4^\circ < i < 10^\circ$). We remark, however, a dearth of large inclination objects. This deficit is intriguing and unexplained, in particular given that the raw simulations of the Nice model (namely those in which the planets are not forced to migrate, but are let free to respond to their interactions with massive planetesimals) produce objects captured in the classical belt or in the detached population with inclinations up to 50° (see Fig. 3 in the *Chapter* by *Gomes et al.*). In general, we would expect an inclination distribution in the hot population that is equivalent to that of *Gomes* (2003), or even more excited. In fact, as pointed out in *Lykawka and Mukai* (2007b), the inclinations in the scattered disk, from which the hot population is derived, are restricted to be less than $\sim 40^\circ$ by the conservation of the Tisserand parameter with respect to Neptune, which holds if the planet is on a quasi-circular orbit as in the simulations of *Gomes* (2003). In the Nice model, the eccentricity of Neptune breaks the conservation of the Tisserand parameter, and hence, in principle, inclinations can be larger.

The results of the simulations based on the Nice model also provide a qualitative explanation for the observed correlations between inclination and physical properties. The particles that are trapped in the cold classical belt come, almost exclusively, from the outermost parts of the planetesimal disk — in particular beyond 29 AU. Conversely, a significant fraction of those trapped in the hot population come from the inner disk. Thus, if one assumes that the largest objects could form only in the inner part of the disk,then these objects can only (or predominantly) be found in the hot population. Similarly, if one assumes that (for some unknown reason) the objects from the outer part of the disk are red and those from the inner part are gray, the cold population would be composed almost exclusively of red objects, whereas the hot population would contain a mixture of red and gray bodies.

The simulations in *Levison et al.* (2007) show that 50 to 130 particles out of 60,000 are trapped in the classical belt

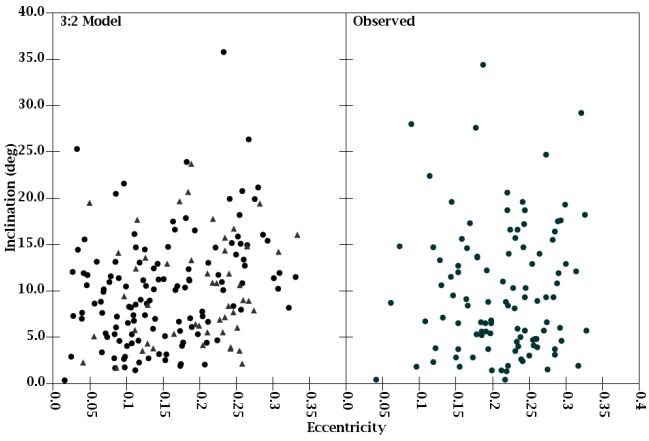

Fig. 11.— The eccentricity–inclination distribution of the Plutinos. Left panel: the simulated distribution; black dots refer to particles from the outer disk and gray triangles to particles from the inner disk. Right panel: the observed distribution. The relative deficit of observed Plutinos at low eccentricity with respect to the model is probably due to observational biases and to the criterion used to select 'resonant objects' from the simulation (see *Levison et al.*, 2007).

(cold and hot populations together in roughly equal proportion). According to the Nice model, the original planetesimal disk contained 35 $M_\oplus$, thus this model predicts that the classical Kuiper belt should currently contain between ~ 0.02 and $\sim 0.08 M_\oplus$, in good agreement from observational estimates. Of course, to be viable, the model needs to explain not only the total mass of the belt, but also the total number of bright, detectable bodies. It does this quite nicely if one assumes that the original disk size-distribution is similar to the one currently observed. As we explained in section 6.1, this is consistent with other constraints like the formation of the Pluto-Charon binary. Thus, the Nice model explains, for the first time, the mass deficit of the Kuiper belt and the ratio between the hot and the cold population, in the framework of an initial planetesimal size distribution that fulfills all the constraints enumerated in section 6.

Finally, the Nice model reproduces in a satisfactory way the orbital distributions of the populations in the main mean motion resonances with Neptune. Fig. 11 compares the (e, i) distribution of the Plutinos obtained in one of *Levison et al. (2007)*'s simulations, against the observed distribution. The overall agreement is quite good. In particular, this is the first model that does not produce an overabundance of resonant objects with low inclinations.

Moreover, the left panel of Fig, 11 uses different symbols to indicate the particles captured from the inner ($a < 29$ AU) and the outer ($a > 29$ AU) parts of the disk. As one sees, the particles are very well mixed, which is in agreement with the absence of correlations between colors and inclinations among the Plutinos. Conversely, a very strong correlation was expected in the original *Gomes* (2003) scenario because a large number of low-inclination bodies were captured from the cold disk. The reason that the Nice model is so much more successful than previous models is that the 2:3 resonance cannot capture any objects via the mechanism of *Malhotra* (1995). This is due to the fact that the resonance is already beyond the disk's outer edge at the beginning of the simulation (i.e. after the last encounter of Neptune with Uranus). We believe that this success strongly supports that idea of a planetesimal disk truncated at 30–35 AU and of a 'jump' of Neptune towards the outer edge of the disk.

As for the higher order resonances beyond 50 AU, the simulations of *Levison et al.* (2007) produce populations with moderate libration amplitudes and inclinations consistent with observations, thus satisfying the constraint posed by *Lykawka and Mukai* (2007a).

In summary, the strength of the Nice model is that it is able to explain *all* the intriguing properties of the Kuiper belt, at least at a semi-quantitative level, in the framework of a single, unique event. That the same scenario also explains the orbital architecture of the giant planets, the Trojans of both Jupiter and Neptune, and the LHB is, of course, a non-negligible additional plus that should give credence to the model.

Of course, the Nice model is not perfect. As we have seen above, the simulations thus far performed have not been able to simultaneously produce: 1) the very highest inclinations that we see, and 2) a cold belt that is cold enough. The numerical simulations contain some simplifications which might effect the results. In particular, mutual collisions and collective gravitational effects among the planetesimals are neglected. Moreover, as discussed in *Levison et al* (2007), only a subset of the evolutions of the giant planets observed in the simulations of the *Tsiganis et al.* (2005) will produce a cold classical belt. Some experiments overly excite inclinations so that a cold belt is not formed, despite producing good final planetary orbits. Nonetheless, we feel that the Nice model's strengths outweigh it weaknesses, particularly given that other models of Kuiper belt formation have had much more limited success at reproducing the observations.

7.1. Other planetary instability models

The Nice model is not the first model to make use of a temporary dynamical instability of the giant planet system (and probably also not the last one!).

Thommes et al. (1999) proposed that Uranus and Neptune formed in between the orbits of Jupiter and Saturn. They were subsequently destabilized and scattered onto orbits with larger semi-major axis and eccentricities. The dynamical excitation was eventually damped by the dynamical friction exerted by a massive planetesimal disk, and the planets achieved stable orbits. Their simulations showed an interesting sculpting of the (a, e) distribution in the region corresponding to the classical Kuiper belt. However, the planetesimal disk was extended to 60 AU. Thus, no outer edge was produced at the 1:2 resonance with Nep-

tune and there was not enough mass depletion in the Kuiper belt. Moreover, since Uranus and Neptune started between Jupiter and Saturn they suffered much stronger encounters with the gas giants than occurred in the Nice model. As a result, the planetesimal disk needed to be much more massive — so massive that if the simulations had been run to completion, Neptune would have migrated well beyond 30 AU.

Chiang et al. (2006) have recently speculated on a scenario based on recent work by *Goldreich et al*. (2004a,b), who, from analytic considerations, predicted the formation of 5 planets between 20 and 40 AU. These planets remained stable during their formation because their orbits were continuously damped by the dynamical friction exerted by a disk of planetesimals that contained more mass than the planetary system. These planetesimals were very small (sub-meter in size) and thus remain dynamically cold due to collisional damping. When the planets reached Neptune-mass, the mass of the planets and the mass of the disk became comparable, so that the planets became unstable. *Goldreich et al*. conjectured that 3 of the 5 planets were ejected and the two remaining ones stabilized on orbits comparable to those of Uranus and Neptune.

Chiang et al. suggested that at the time of the instability, the disk contained two populations: one made up of ~ 100 km objects and one consisting of sub-meter objects. The current Kuiper belt structure would be the result of the orbital excitation suffered during the multi-planet instability. The hot population would be made up of the larger objects which were permanently excited during the instability. In contrast the smallest planetesimals would suffer a significant amount of collisional damping, which would have led to the eventual accretion of the cold population. Numerical simulations made by *Levison and Morbidelli* (2007) with a new code that accounts for a planetesimal disk with strong internal collisional damping, invalidate the *Goldreich et al*. proposal. It is found that a system of 5 unstable Neptune-mass planets systematically leads to a system with more than 2 planets, spread in semi-major axis well beyond 30 AU. Thus, the architecture of the solar planetary system is inconsistent with *Goldreich et al*.'s idea.

8. Conclusions and Discussion

In this chapter we have tried to understand which kind of solar system evolution could have produced the most important properties of the Kuiper belt: its mass deficit, its outer edge, the co-existence of a cold and a hot classical population with different physical properties, and the presence of resonant populations. We have proceeded by basic steps, trying to narrow the number of possibilities by considering one Kuiper belt feature after the other, and starting from the most accepted dynamical process (planet migration) and eventually ending with a more extravagant one (a temporary instability of the giant planets).

We have converged to a basic scenario with three ingredients: the planetesimal disk was truncated close to 30 AU and the Kuiper belt was initially empty; the size distribution in the planetesimal disk was similar to the current one in the Kuiper belt, but the number of objects at each size was larger by a factor of $\sim 1,000$; the Kuiper belt objects are just a very small fraction of the original planetesimal disk population and were implanted onto their current orbit from the disk during the evolution of the planets. A temporary high-eccentricity phase of Neptune, when the planet was already at ~ 28 AU –as in the Nice model– seems to be the best way to implant the cold population.

The mass deficit problem is the main issue that drove us to this conclusion. In particular, we started from the consideration that, if a massive disk had extended into the Kuiper belt, neither collisional grinding nor dynamical ejection could have depleted its mass to current levels. Dynamical ejection seems to be excluded by the constraint that Neptune did not migrate past 30 AU. Collisional grinding seems to be excluded by the arguments that the size distribution was about the same everywhere in the disk and that $\sim 1,000$ Pluto-size bodies had to exist in the planetary region.

Is there a flaw in this reasoning? Are we really sure that the cold population did not form in situ? The argument that the size distribution of the in-situ population should be similar to that in the region spanned by Neptune's migration neglects possible effects due to the presence of an edge. After all, an edge is a big discontinuity in the size and mass distribution, so that it may not be unreasonable that the region adjacent to the edge had very different properties from the region further away from the edge.

Our view of the Kuiper belt evolution could radically change if a model of accretion were developed that produces a disk of planetesimals with a size distribution that changes drastically with distance, such that (a) beyond 45 AU all objects are too small to be detected by telescope surveys, (b) in the 35–45 AU region the distribution of the largest objects is similar to that observed in the current cold population while most of the mass is contained in small bodies, and (c) within 35 AU most of the mass is contained in large bodies and the size distribution culminating with $\sim 1,000$ Pluto-sized objects. If this were the case, the disk beyond 35 AU could lose most of its mass by collisional grinding before the beginning of Neptune's migration, particularly if the latter was triggered late as in our LHB scenario (see sect. 3.4 of the *chapter* by Kenyon et al.). Within 35 AU, because of the different size distribution, collisional grinding would have been ineffective (*Charnoz and Morbidelli*, 2007). Therefore, at the time of the LHB, the system would have been similar to the one required by the Nice model, in that Neptune would have seen an effective edge in the planetesimal mass distribution that would have kept it from migrating beyond 30 AU.

Whether the spatial variation we described above of the size distribution in the planetesimal disk is reasonable or not is beyond our current understanding. The *chapter* by Kenyon et al. in this book, nicely shows that the coagulation/erosion process is always on the edge of an instability. In fact, the dispersion velocity of the small bodies is

of the order of the escape velocity from the largest bodies. Depending on the details of the collisional cascade (see sect. 3.5 in that chapter) the dispersion velocity can be slightly smaller than the escape velocities (favoring the accretion of a large number of massive bodies and producing a top-heavy size distribution which does not allow an effective collisional grinding), or can be slightly larger (stalling runaway accretion and leaving most of the mass in small, easy to break bodies). Perhaps, the inner part of the disk was in the first regime and the outer part was in the second one, with a relatively sharp transition zone between the two parts. More work is needed to clarify the situation, with a close collaboration between experts of accretion and of dynamical evolution.

From a purely dynamical point of view, the Nice model is not inconsistent with the existence of a local, low mass Kuiper belt population, extended up to 44–45 AU. In fact, Fig. 12 compares the (a, e) distribution observed in the classical belt with $q > 38$ AU (bottom panel) with the one that the Nice model predicts assuming that the disk was truncated at 34 AU (top panel, enlargment of the left panel in Fig. 9) or assuming that the disk was truncated at 44 AU (middle panel). The two model distributions are statistically equivalent, and are both very similar to the observed distribution. In the case where the outer edge was placed at 44–45 AU about 7% of the particles initially in the Kuiper belt ($a > 40$ AU, $q > 38$ AU) remain there, although their orbits have been modified. The others escape to larger eccentricities during the phase when the Kuiper belt is globally unstable, discussed in sect. 7. If 90% of the local mass escapes, the local belt had to have been signficantly depleted before the time of the LHB, probably accounting for only a few tens of an Earth mass, otherwise, presumably (see sect. 6.1), Neptune would have been driven past 30 AU.

We end this chapter by encouraging observers to attempt to probe the regions beyond 50 AU. In particular, even if the absence of a population of objects similar to that in the 40–50 AU region is now secure, nothing is known on the possible existence of small objects. Recent claims on a large number of stellar occultation events by distant ~ 100m objects (*Roques et al.*, 2006; *Chang et al.*, 2006; *Georgevits*, 2006) may suggest, if confirmed (see *Jones et al.* 2006 for a rebuttal of *Chang et al.* results), the existence of an extended disk of small planetesimals that did not grow to directly detectable sizes. If true, this would give us extremely valuable information on the origin of the Kuiper belt edge. The model by Weidenschilling predicts the existence of an extended disk of exclusively small bodies, although of sizes up to $\sim 1m$ rather than ~ 100 m (see Fig. 5). Conversely, other models on edge formation, such as the disk stripping by passing stars, photo-evaporation or turbulent stirring, would predict the total absence of objects, of any size. Therefore we encourage the pursuit of stellar occultation programs, until the real situation is clarified.

So far, the Kuiper belt has taught a lot to us about the evolution of the planets. Planet migration, for instance, had been totally overlooked despite the pioneer work by Fernandez and Ip, until the Kuiper belt was discovered. Moreover, as we mentioned above, we can find in the Kuiper belt further evidence that the giant planets passed through a temporary phase of violent instability. But, the Kuiper belt can do more. It can potentially teach us about planetesimal formation and the growth of larger objects because the objects that inhabit it most likely probe different regions of the proto-planetary disk where accretion proceeded in very different ways. Thus, it is a dreamed-of laboratory to test and calibrate the accretion models. This is probably the main venue for the future.

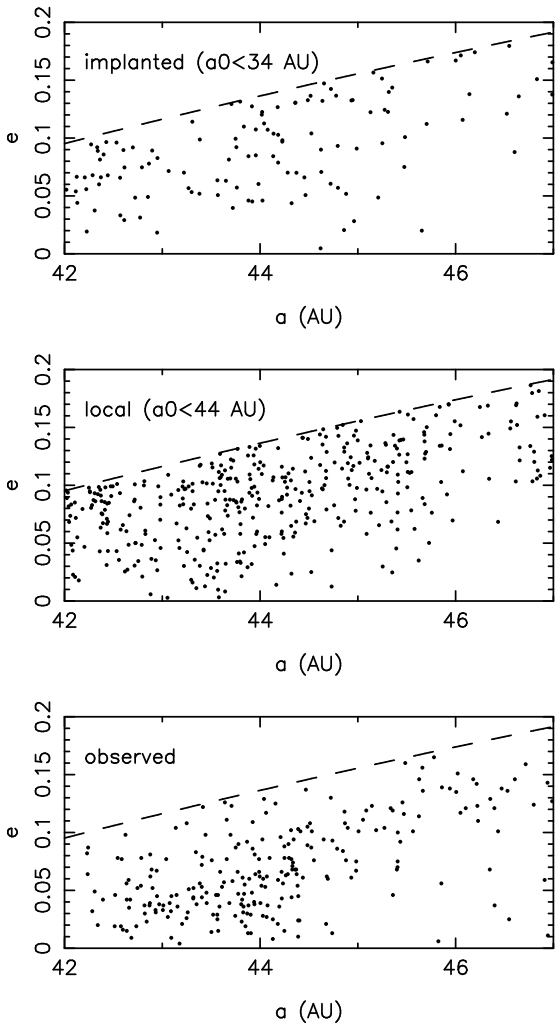

Fig. 12.— The semi-major axis vs. eccentricity distribution in the classical belt ($q > 38$ AU). Top panel: the distribution of the objects that originated within 34 AU, implanted in the Kuiper belt at the time of the LHB. Middle panel: the distribution of the bodies assuming the disk originally extended to 44 AU. Bottom panel: the observed distribution.

H.F.L. thanks NASA's *Origins* and *Planetary Geology and Geophysics* programs for supporting his involvement in the research related to this Chapter. A.M. is also grateful to the French National Council of Scientific Research (CNRS)

and National Programme of Planetology (PNP) for support. RSG thanks the Brasilian National Council for Science and Technology (CNPq) for support.

REFERENCES

Adams, F. C., Hollenbach, D., Laughlin, G., Gorti, U. 2004. Photoevaporation of Circumstellar Disks Due to External Far-Ultraviolet Radiation in Stellar Aggregates. Astrophysical Journal 611, 360-379.

Agnor, C. B., Hamilton, D. P. 2006. Neptune's capture of its moon Triton in a binary-planet gravitational encounter. Nature 441, 192-194.

Allen, R.L., Bernstein, G.M., Malhotra, R. 2001. The edge of the solar system. *Astroph. J.*, **549**, L241-L244.

Allen, R.L., Bernstein, G.M., Malhotra, R. 2002. Observational Limits on a Distant Cold Kuiper Belt. *Astron. J.*, **124**, 2949-2954.

Augereau, J.-C., Beust, H. 2006. On the AU Microscopii debris disk. Density profiles, grain properties, and dust dynamics. Astronomy and Astrophysics 455, 987-999.

Benz, W., Asphaug, E. 1999. Catastrophic Disruptions Revisited. Icarus 142, 5-20.

Barkume, K. Brown, M. and Schaller, E.L. 2006. Discovery of a colisional family in the Kuiper belt. BAAS, 38, 565.

Beauge, C. 1994. Asymmetric liberations in exterior resonances. Celestial Mechanics and Dynamical Astronomy 60, 225-248.

Bernstein, G. M., Trilling, D. E., Allen, R. L., Brown, M. E., Holman, M., Malhotra, R. 2004. The Size Distribution of Trans-Neptunian Bodies. Astronomical Journal 128, 1364-1390.

Brown M. 2001. The Inclination Distribution of the Kuiper Belt. *Astron. J.*, **121**, 2804-2814.

Brown, M. E., Trujillo, C. A., Rabinowitz, D. L. 2005. Discovery of a Planetary-sized Object in the Scattered Kuiper Belt. Astrophysical Journal 635, L97-L100.

Brunini A., Melita M. 2002. The existence of a planet beyond 50 AU and the orbital distribution of the classical Edgeworth Kuiper belt objects. *Icarus*, **160**, 32-43.

Canup, R. M., Ward, W. R. 2006. A common mass scaling for satellite systems of gaseous planets. Nature 441, 834-839.

Charnoz, S. and Morbidelli, A. 2007. Coupling dynamical and collisional evolution of small bodies. II: Forming the Kuiper Belt, the scattered disk and the Oort cloud. Icarus in press.

Chiang., E., Lithwick, Y., Murray-Clay, R., Buie, M., Grundy, W. and Holman, M. 2006. A brief history of the trans-Neptunian space. In *Protostars and planets V*, (B. Reipurth et al. eds.), University Arizona Press, Tucson, Az.

Chirikov, B. V. 1960. Resonance processes in magnetic traps. Journal of Plasma Physics 1, 253-260.

Davis D. R., Farinella P. 1998, Collisional Erosion of a Massive Edgeworth-Kuiper Belt: Constraints on the Initial Population. In *Lunar Planet. Science Conf.* **29**, 1437–1438.

Davis D. R., Farinella P. 1997. Collisional Evolution of Edgeworth-Kuiper Belt Objects. *Icarus*, **125**, 50–60.

Dermott, S. F., Murray, C. D. 1983. Nature of the Kirkwood gaps in the asteroid belt. Nature 301, 201-205.

Duncan, M. J., Levison, H. F., Budd, S. M. 1995, The long-term stability of orbits in the Kuiper belt, *Astron. J.*, **110**, 3073–3083.

Duncan, M. J., Levison, H. F. 1997. A scattered comet disk and the origin of Jupiter family comets. Science 276, 1670-1672.

Emel'yanenko, V. V., Asher, D. J., Bailey, M. E. 2003. A new class of trans-Neptunian objects in high-eccentricity orbits. Monthly Notices of the Royal Astronomical Society 338, 443-451.

Fernandez, J. A., Ip, W.-H. 1984. Some dynamical aspects of the accretion of Uranus and Neptune - The exchange of orbital angular momentum with planetesimals. Icarus 58, 109-120.

Georgevits, G. 2006. Detection of Small Kuiper Belt Objects by Stellar Occultation. AAS/Division for Planetary Sciences Meeting Abstracts 38, #37.07.

Gladman, B., Kavelaars, J.J., Petit, J.M., Morbidelli, A., Holman, M.J., Loredo, Y., 2001. The structure of the Kuiper belt: Size distribution and radial extent. *Astron. J.*, **122**, 1051-1066.

Goldreich, P., Lithwick, Y., Sari, R. 2004a. Final Stages of Planet Formation. Astrophysical Journal 614, 497-507.

Goldreich, P., Lithwick, Y., Sari, R. 2004b. Planet Formation by Coagulation: A Focus on Uranus and Neptune. Annual Review of Astronomy and Astrophysics 42, 549-601.

Gomes R. S. 2000. Planetary Migration and Plutino Orbital Inclinations *Astron. J.*, **120**, 2695-2707.

Gomes, R. S. 2003. The origin of the Kuiper Belt high-inclination population. Icarus 161, 404-418.

Gomes, R. S., Morbidelli, A., Levison, H. F. 2004. Planetary migration in a planetesimal disk: why did Neptune stop at 30 AU?. Icarus 170, 492-507.

Gomes, R., Levison, H. F., Tsiganis, K., Morbidelli, A. 2005. Origin of the cataclysmic Late Heavy Bombardment period of the terrestrial planets. Nature 435, 466-469.

Grundy, W. M., Noll, K. S., Stephens, D. C. 2005. Diverse albedos of small trans-neptunian objects. Icarus 176, 184-191.

Hahn, J. M., Malhotra, R. 1999. Orbital Evolution of Planets Embedded in a Planetesimal Disk. Astronomical Journal 117, 3041-3053.

Hahn, J. M., Malhotra, R. 2005. Neptune's Migration into a Stirred-Up Kuiper Belt: A Detailed Comparison of Simulations to Observations. Astronomical Journal 130, 2392-2414.

Henrard J. 1982. Capture into resonance - An extension of the use of adiabatic invariants. *Cel. Mech.*, **27**, 3–22.

Hollenbach, D., Adams, F. C. 2004. Dispersal of Disks Around Young Stars: Constraints on Kuiper Belt Formation. ASP Conf. Ser. 324: Debris Disks and the Formation of Planets 324, 168.

Holman, M. J., Wisdom, J. 1993. Dynamical stability in the outer solar system and the delivery of short period comets. Astronomical Journal 105, 1987-1999.

Ida S., Larwood J., Burkert A. 2000. Evidence for Early Stellar Encounters in the Orbital Distribution of Edgeworth-Kuiper Belt Objects. *Astroph. J.*, **528**, 351–356.

Jones, T. A., Levine, A. M., Morgan, E. H., Rappaport, S. 2006. Millisecond Dips in Sco X-1 are Likely the Result of High-Energy Particle Events. The Astronomer's Telegram 949, 1.

Kenyon, S.J., Luu, J.X. 1998. Accretion in the early Kuiper belt: I. Coagulation and velocity evolution. *Astron. J.*, **115**, 2136-2160.

Kenyon, S.J., Luu, J.X. 1999a. Accretion in the early Kuiper belt: II. Fragmentation. *Astron. J.*, **118**, 1101-1119.

Kenyon, S.J., Luu, J.X. 1999b. Accretion in the early outer solar system. *Astrophys. J*, **526**, 465-470

Kenyon S.J. and Bromley B.C. 2002. Collisional Cascades in Planetesimal Disks. I. Stellar Flybys. *Astron. J.*, **2002**, 1757-1775.

Kenyon, S. J., Bromley, B. C. 2004a. The Size Distribution of Kuiper Belt Objects. Astronomical Journal 128, 1916-1926.

Kenyon, S. J., Bromley, B. C. 2004b. Stellar encounters as the

origin of distant Solar System objects in highly eccentric orbits. Nature 432, 598-602.

Knežević Z., Milani A., Farinella P., Froeschlé Ch. and Froeschlé C. 1991. Secular resonances from 2 to 50 AU. *Icarus*, **93**, 316-330.

Kobayashi H., Ida S. 2001. The Effects of a Stellar Encounter on a Planetesimal Disk. *Icarus*, **153**, 416-429.

Kobayashi, H., Ida, S., Tanaka, H. 2005. The evidence of an early stellar encounter in Edgeworth Kuiper belt. Icarus 177, 246-255.

Kuchner M.J., Brown M.E., Holman M. 2002. Long-Term Dynamics and the Orbital Inclinations of the Classical Kuiper Belt Objects. *Astron. J.*, **124**, 1221-1230.

Levison H.F., Stern S.A. 2001. On the Size Dependence of the Inclination Distribution of the Main Kuiper Belt. Astronomical J., **121**, 1730-1735.

Levison, H. F., Morbidelli, A. 2003. The formation of the Kuiper belt by the outward transport of bodies during Neptune's migration. Nature 426, 419-421.

Levison, H. F., Morbidelli, A., Dones, L. 2004. Sculpting the Kuiper Belt by a Stellar Encounter: Constraints from the Oort Cloud and Scattered Disk. Astronomical Journal 128, 2553-2563.

Levison, H. F., Morbidelli, A., Gomes, R. and Backman, D. 2006. Planet migration in planetesimal disks. In *Protostars and planets V*, (B. Reipurth et al. eds.), University Arizona Press, Tucson, Az.

Levison, H. F. and Morbidelli, A. 2007. Neptune-mass planets did not form in the Kuiper belt. Icarus, in press.

Levison H. F., Morbidelli, A., Gomes, R. and Tsiganis, K. 2007 Origin of the structure of the Kuiper Belt during a Dynamical Instability in the Orbits of Uranus and Neptune. Icarus, submitted.

Lykawka, P. S. and Mukai, T. 2007a. Evidence for an excited Kuiper belt of 50 AU radius in the first Myr of solar system history. Icarus, in press.

Lykawka, P. S. and Mukai, T. 2007b. Dynamical classification of trans-Neptunian objects: Probing their origin, evolution and interrelation. Icarus, in press.

Malhotra, R. 1993. The Origin of Pluto's Peculiar Orbit. Nature 365, 819.

Malhotra, R. 1995. The Origin of Pluto's Orbit: Implications for the Solar System Beyond Neptune. Astronomical Journal 110, 420.

Malhotra, R. 1996. The Phase Space Structure Near Neptune Resonances in the Kuiper Belt. Astronomical Journal 111, 504.

Melita M., Larwood J., Collander-Brown S, Fitzsimmons A., Williams I.P., Brunini A. 2002. The edge of the Edgeworth-Kuiper belt: stellar encounter, trans-Plutonian planet or outer limit of the primordial solar nebula? In *Asteroid, Comet, Meteors*, ESA Spec. Publ. series, 305-308.

Message, P. J. 1958. Proceedings of the Celestial Mechanics Conference: The search for asymmetric periodic orbits in the restricted problem of three bodies. Astronomical Journal 63, 443.

Morbidelli, A., Henrard, J. 1991. The main secular resonances nu6, nu5 and nu16 in the asteroid belt. Celestial Mechanics and Dynamical Astronomy 51, 169-197.

Morbidelli A., Thomas F. and Moons M. 1995. The resonant structure of the Kuiper belt and the dynamics of the first five trans-Neptunian objects. *Icarus*, **118**, 322.

Morbidelli A., Valsecchi G. B. 1997. Neptune scattered planetesimals could have sculpted the primordial Edgeworth–Kuiper belt, *Icarus*, **128**, 464–468.

Morbidelli A., 2002. *Modern Celestial Mechanics: aspects of Solar System dynamics*, in "Advances in Astronomy and Astrophysics", Taylor & Francis, London.

Morbidelli, A., Levison, H. F. 2004. Scenarios for the Origin of the Orbits of the Trans-Neptunian Objects 2000 CR_{105} and 2003 VB_{12} (Sedna). Astronomical Journal 128, 2564-2576.

Morbidelli, A., Levison, H. F., Tsiganis, K., Gomes, R. 2005. Chaotic capture of Jupiter's Trojan asteroids in the early Solar System. Nature 435, 462-465.

Murray-Clay, R. A., Chiang, E. I. 2006. Brownian Motion in Planetary Migration. Astrophysical Journal 651, 1194-1208.

Nagasawa M., Ida S. 2000. Sweeping Secular Resonances in the Kuiper Belt Caused by Depletion of the Solar Nebula. *Astron. J.*, **120**, 3311–3322.

Nesvorný D. and Roig F. 2000. Mean motion resonances in the trans-neptunian region: Part I: The 2:3 resonance with Neptune. *Icarus*, 148, 282-300.

Nesvorný D. and Roig F. 2001. Mean motion resonances in the trans-neptunian region: Part II: the 1:2, 3:4 and weaker resonances. *Icarus*, 150, 104-123.

Petit, J.-M., Morbidelli, A., Chambers, J. 2001. The Primordial Excitation and Clearing of the Asteroid Belt. Icarus 153, 338-347.

Roques, F., and 17 colleagues 2006. Exploration of the Kuiper Belt by High-Precision Photometric Stellar Occultations: First Results. Astronomical Journal 132, 819-822.

Ruden, S. P., Pollack, J. B. 1991. The dynamical evolution of the protosolar nebula. Astrophysical Journal 375, 740-760.

Sekiya, M. 1983. Gravitational instabilities in a dust-gas layer and formation of planetesimals in the solar nebula. Progress of Theoretical Physics 69, 1116-1130.

Sheppard, S. S., Trujillo, C. A. 2006. A Thick Cloud of Neptune Trojans and Their Colors. Science 313, 511-514.

Stern, S. A. 1991, On the number of planets in the outer solar system - Evidence of a substantial population of 1000-km bodies, Icarus, 90, 271–281

Stern, S. A. 1996, On the Collisional Environment, Accretion Time Scales, and Architecture of the Massive, Primordial Kuiper Belt., *Astron. J.*, **112**, 1203–1210.

Stern, S. A., Colwell, J. E. 1997a, Accretion in the Edgeworth-Kuiper Belt: Forming 100-1000 KM Radius Bodies at 30 AU and Beyond. *Astron. J.*, **114**, 841-849.

Stern, S. A., Colwell, J. E. 1997b, Collisional Erosion in the Primordial Edgeworth-Kuiper Belt and the Generation of the 30-50 AU Kuiper Gap, *Astroph. J.*, **490**, 879–885.

Stern, S. A., Weissman, P. R. 2001. Rapid collisional evolution of comets during the formation of the Oort cloud. Nature 409, 589-591.

Stone, J. M., Gammie, C. F., Balbus, S. A. and Hawley, J. F. in Protostars and Planets IV (eds Mannings, V., Boss, A. P. and Russell, S. S.) 589 (Univ. Arizona Press, Tucson, 1998)

Thommes, E. W., Duncan, M. J., Levison, H. F. 1999. The formation of Uranus and Neptune in the Jupiter-Saturn region of the Solar System. Nature 402, 635-638.

Trujillo C.A., Brown M.E. 2001. The Radial Distribution of the Kuiper Belt. *Astroph. J*, **554**, 95-98.

Trujillo, C. A., Brown, M. E. 2003. The Caltech Wide Area Sky Survey. Earth Moon and Planets 92, 99-112.

Tsiganis, K., Gomes, R., Morbidelli, A., Levison, H. F. 2005. Origin of the orbital architecture of the giant planets of the Solar System. Nature 435, 459-461.

Youdin, A. N., Shu, F. H. 2002. Planetesimal Formation by Gravitational Instability. Astrophysical Journal 580, 494-505.

Weidenschilling S. 2003. Formation of Planetesimals/Cometesimals in the Solar nebula. in *Comet II*, Festou et al. eds., University Arizona Press, Tucson, Az. 97–104.

Williams, J. G., Faulkner, J. 1981. The positions of secular resonance surfaces. Icarus 46, 390-399.

Wisdom, J. 1980. The resonance overlap criterion and the onset of stochastic behavior in the restricted three-body problem. Astronomical Journal 85, 1122-1133.